Journal of Applied Electrochemistry **30**: 429–437, 2000.

Electrochemical investigation of the codeposition of SiC and SiO_2 particles with nickel

P. NOWAK[1]*, R.P. SOCHA[1], M. KAISHEVA[2], J. FRANSAER[3], J.-P. CELIS[3] and Z. STOINOV[4]
[1]*Polish Academy of Sciences, Institute of Catalysis and Surface Chemistry, ul. Niezapominajek 1, 30239 Kraków, Poland;*
[2]*University of Sofia, Faculty of Chemistry, Department of Physical Chemistry, 1, J. Bourchier Bul., 1126 Sofia, Bulgaria;*
[3]*Department of Metallurgy and Materials Engineering, Katholieke Universiteit Leuven, B-3001 Heverlee, Belgium;*
[4]*Bulgarian Academy of Sciences, Central Laboratory of Electric Power Sources, Sofia 1126, Bulgaria*
*(*author for correspondence)*

Received 28 April 1999; accepted in revised form 2 September 1999

Key words: composite coatings, electrochemical impedance spectroscopy, nickel electrodeposition, particle codeposition, silicon carbide

Abstract

The use of electrochemical impedance spectroscopy (EIS) for the *in situ* control of the electrolytic codeposition of Ni/SiO_2 and Ni/SiC was investigated. An attempt was made to clarify why silica particles hardly codeposit in comparison to silicon carbide particles. It was found that the presence of SiO_2 and SiC particles influences the metal deposition process in different ways. SiC particles that are being embedded in the growing metal layer cause an apparent decrease in the electrode surface area, probably due to blocking off a part of the surface by partly engulfed particles. In the case of SiO_2 particles, which embed in the metal matrix to a very limited extent, no blocking was observed. It was found that the presence of particles in the solution causes an apparent increase in the electrode surface area, probably due to increased surface roughness.

1. Introduction

Solid particles suspended in a plating bath can adhere to the cathode during electrolysis and, under certain conditions, be embedded in the growing metal layer. This phenomenon can lead to the contamination of the metal deposit during electrorefining, but is also the basis for composite plating technology [1–9]. After recognition that electrophoresis, proposed initially by Withers [10] as a mechanism of codeposition, cannot be operative in highly concentrated plating solutions, mechanical entrapment was considered for some time [11, 12]. It was then found that certain cations (e.g., thallium), anions (e.g., fluoroborate) or organic additives (some amines) have an influence on the codeposition [2, 13]. A first mathematical description of the electrolytic codeposition by Guglielmi [14] was based on a two-step codeposition mechanism. Guglielmi assumed that particles are first reversibly adsorbed on the electrode surface. These loosely adsorbed particles are then embedded in an electrochemical step. The adsorption of metal cations onto the particle surface was subsequently considered [13, 15–20]. Considering the reduction of the metal ions present on the surface of particles as the key step in codeposition, Celis et al. [21] derived an equation which allows a prediction on the degree of codeposition for systems of defined hydrodynamics (e.g., rotating disc electrode). An attempt to develop a predictive model was undertaken by Fransaer et al. [22]. The number of particles reaching the surface of a rotating disc electrode was calculated using a trajectory analysis, taking into account all forces acting on a particle. Hydration forces were invoked to explain the observed dependence of deposition rate on the electrode potential. These hydration forces hinder particles to approach closely the electrode surface. Strong repulsion between hydrated surfaces at short separation distances in concentrated solutions of inorganic electrolytes has already been reported in the literature [23].

Watson and Walters [25] and Watson [26] investigated the codeposition of chromium particles and silicon carbide particles with nickel by EIS, whereas Yeh and Wan [27] studied the codeposition of silicon carbide particles with nickel. Watson and Walters [25, 26] observed two capacitive loops and two inductive loops in the impedance Nyquist plots. One of the capacitive loops, at very high frequency (10^4 Hz $< f < 10^5$ Hz) was interpreted as the electrical double layer (EDL) capacitance in parallel with a charge transfer resistance and the other, in the frequency range of 10 Hz $< f <$ 10^4 Hz, was related to an adsorption step pseudo-capacitance in parallel to an adsorption step resistance.

Based on a graphical analysis of these EIS data, an EDL capacitance of 2–4 μF cm^{-2} was calculated. This capacitance is at least one order of magnitudes lower than values reported earlier, whereas the pseudo-capacitances were of the same order of magnitudes as the earlier reported EDL capacitances [28–33]. Watson [26] reported that the introduction of SiC to the solution at constant potential causes a significant increase in current. However at the same time, an increase in charge transfer resistance was observed. This is puzzling because an increase in current should rather be accompanied by a decrease in charge transfer resistance.

Yeh and Wan [27] did not observe the high-frequency capacitive loop and interpreted the capacitive loop in the frequency range 10 Hz $< f <$ 10^4 Hz as the charge transfer resistance in parallel with EDL capacitance. They assumed the same equivalent electrical circuit (EEC) as Watson and Walters [26], and applied the 'simulate-and-compare' method for the interpretation of their EIS data. Again the interpretation of the impedance measurements by Yeh and Wan is unclear. The impedance spectra with well developed inductive loop cannot be simulated by an EEC composed of resistors and capacitors only, assumed by those authors. Also, the values of the adsorption step pseudo-capacitance given by Yeh and Wan [27] are two orders of magnitudes higher than those reported by Watson and Walters. Furthermore, neither Watson and Walters [25, 26] nor Yeh and Wan [27] analysed the SiC content of their deposits. Strong influence of the presence of SiC particles in the solution on the electrode impedance during nickel electrodeposition was also reported by Benea and Carac [34].

As previous impedance spectroscopy studies led to contradictory results, the effect of solid particles suspended in an electrolyte on the impedance of the interface between the electrode and the plating solution was reconsidered in this work. Two systems were investigated: nickel/silicon carbide and nickel/silica. There are many reports on the codeposition of SiC with nickel [26, 27, 34–36]. SiC is known to codeposit in large amounts with metals. On the contrary, the codeposition of silica with metals occurs to a rather limited extent [36–39]. Amounts of codeposition higher than 1 wt% (without additives) has not been reported. A codeposition of silica with zinc up to 6%, was observed only under conditions where the simultaneous precipitation of $Zn(OH)_2$ occurred [40, 41].

2. Experimental details

A Watt's bath containing 300 g dm^{-3} $NiSO_4.6H_2O$, 35 g dm^{-3} $NiCl_2.6H_2O$ and 40 g dm^{-3} H_3BO_3 was used. The pH was regulated between 2 and 4 by adding either H_2SO_4 or NaOH. The experiments were performed at 55 °C. Analytical reagent grade chemicals and triply distilled water were used. α-SiC particles (Norton, Norway, ref. 15-NLC) with a particle size of 0.6 μm were selected for this study. The silica particles were obtained by grinding high quality quartz sand in a ball mill with iron balls. After grinding, the particles were washed repeatedly in nitric acid and water until no iron was detected in the supernatant liquid, then deslimed and finally dried. The mean diameter of the particles, measured by Coulter Counter, was 1.5 μm. The dispersion of the particle diameter was rather narrow since 90% of the particles had a diameter between 0.4 and 2.5 μm.

Impedance measurements require electrode surfaces which react uniformly. Rotating disc electrodes do not allow a uniform codeposition of particles due to varying hydrodynamic tangential forces with disc radius [22, 35]. Therefore, three different cell geometries were selected for this work. The first cell had a volume of about 1.0 dm^3 with a cathode area of 25 cm^2 placed in the centre of the cell in a vertical position in between two nickel anodes. Agitation by air bubbling was done from the bottom of the cell. Two 65 cm^3 cells of similar geometry but with a smaller electrode surface area were used for impedance measurements. The electrodes used in these cells were metal disks embedded in PTFE, placed in a vertical position in the wall of the cell. The particles were kept in suspension with a magnetic stirrer located at the bottom of the cell. One of these cells contained a stainless steel cathode disc of the area of 1.06 cm^2. In the other cell, the cathode was a gold disc of 1 mm diameter. A reference saturated calomel electrode (SCE) and a counter electrode of pure nickel were used. The reference electrode was placed in a glass arm separated from the main cell, and the counter electrode was placed as far as possible from the cathode in order not to disturb the uniformity of the current flow to the electrode or the particle distribution at the surface. Impedance spectra were measured with a frequency response analyser FRA 1250 and an electrochemical interface ECI 1286 potentiostat (both Schlumberger–Solartron), controlled by a 9000 series 300 Hewlett–Packard computer. All potentials are given with respect to the SCE and after *IR* potential drop correction.

During potentiostatic deposition, the current was registered continuously. The thickness of the Ni layer was derived from the online integrated current and the current efficiency determined in a separate series of experiments. Codeposition experiments were performed in the large cell in the galvanostatic mode to choose the optimal conditions of suspended particle concentration, pH and current density. The amount of codeposited particles was determined by dissolving the coatings in nitric acid and by weighting the amount of particles after filtration. For the cell containing a disc cathode of 1.06 cm^2 surface area the particle content was determined by stripping and weighing the metal layer then dissolving it in nitric acid. The nickel content was determined by titration with EDTA and murexide used as an end point indicator. The particle content was calculated from the difference in the weight of the

deposit and the mass of nickel. Under identical conditions of pH and SiC concentration in solution, the codeposition in that cell was very similar to the one obtained in the larger cell. The chemical analysis of the SiC content was not possible in the cell with the 1 mm diameter gold electrode due to the small mass of composite.

3. Results

3.1. *SiC and SiO_2 codeposition with nickel*

In agreement with the literature, SiO_2 showed only very limited codeposition with nickel, whereas a high codeposition of silicon carbide was obtained (Figure 1) for the same conditions. Differences in codeposition for SiC at pH 3 and 4 were not observed, but the codeposition of SiC at pH 2 was significantly lower. The mechanical properties of the obtained SiC/Ni composite coatings have been presented elsewhere [42].

Watson [26] observed a drop in the current efficiency from 0.99 to 0.46 in the case of a Watts bath containing SiC particles in comparison to a bath without particles. Such an effect was not observed in our experiments. For deposition without particles at a potential of −0.85 V (*IR* corrected) and pH between 2 and 4, the current efficiency was found to be 0.95 ± 0.03 (mean value from nine experiments). This value is typical for nickel electrocrystallization from a Watts bath. Only a slight increase in current efficiency was observed with increase of pH in that range. In the presence of SiC particles (5–150 g dm^{-3}) at pH 3.0, only a slight decrease in the current efficiency to approximately 0.90 at the highest particle concentration was observed. Also, the Tafel slopes in the presence and absence of suspended SiC particles were similar, namely 95 mV (decade)$^{-1}$ for the pure bath and 105 mV (decade)$^{-1}$ for the bath with SiC (Figure 2), the difference being within the range of accuracy of the measurements.

In some previously published papers on potentiostatic codeposition experiments, the effect of particles on the *IR* potential drop in solution was neglected and thus false conclusions were drawn about the influence of particles on the electrode process. For a working electrode in the form of a disc embedded in a plane, the resistance of the solution (R_s) may be estimated from Newman's equation [43]:

$$R_s = \frac{1}{4\kappa a} \tag{1}$$

where κ is the specific solution conductivity and a is the radius of the disc. From the above equation it follows that for a given current density the *IR* potential drop is higher for the electrode of a bigger diameter. Indeed, the *IR* potential drop, estimated from the high frequency part of an impedance spectrum, was always higher in the case of the electrode of the bigger surface area and higher in solutions containing particles, because the specific conductivity of the suspension is lower in comparison to the pure bath. In the cell with the lowest cathode area, the *IR* drop was relatively low, namely ~27 mV at the highest current density used of 60 mA cm^{-2}. The difference in *IR* potential drop between the pure plating bath and the bath containing particles was negligible in that case (less than 3 mV). However, in the case of the cell with a cathode area of 1.06 cm^2, the maximum *IR* potential drop was 310 mV and consequently, the difference in *IR* potential drop for experiments with and without particles was much higher, namely up to 30 mV. So, only in the cell with the smallest cathode area, could the experiments performed at the same measured potential with and without particles be compared directly, since they were performed at the same real electrode potential.

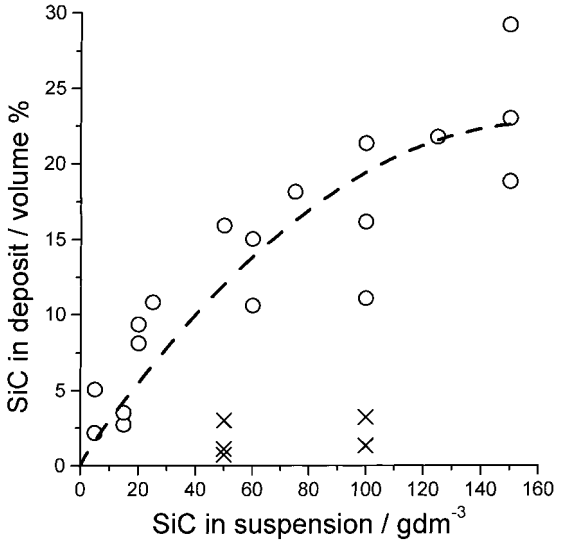

Fig. 1. Amount of α-SiC (○) and SiO_2 (×) particles in the nickel coating as a function of the particle concentration in the suspension. Watts bath operated at 55 °C and pH 3. Stainless steel cathode of 1.06 cm^2. Potential between −0.83 and −0.86 V for different experiments.

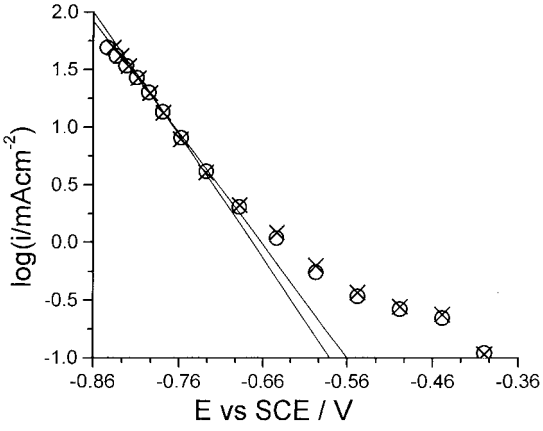

Fig. 2. Tafel plots for a nickel electrode in particle-free nickel Watts bath (×) and in a Watts bath with 100 g dm^{-3} SiC (○). Reported potentials were corrected for *IR* potential drop. Stainless steel disc cathode of 1.06 cm^2, $t = 55$ °C, pH 3.

3.2. *Impedance of the nickel electrode in a pure Watts bath and the bath containing particles*

Impedance spectra for nickel in a particle-free nickel Watts plating bath and in a bath containing 100 g dm^{-3} SiC are shown in Figure 3. The impedance spectra shown correspond to frequencies higher than approximately 0.1 Hz, where the spectrum is determined mainly by the nickel ion discharge reaction; the features connected with discharge of hydrogen ions appear at lower frequencies. These experiments were performed as follows. A 20 μm thick nickel layer was deposited at -0.84 V. The potential was then lowered in steps of about 50 mV to the rest potential of the nickel electrode in the same solution. After every step, the electrode was held for 10 s to stabilise the conditions and the impedance spectrum was recorded. The experiments with SiC were performed in the same way, but after deposition of a 10 μm thick nickel layer from a particle free Watts bath, SiC particles were added to the solution. The first spectrum was recorded after deposition of a second 10 μm thick composite nickel layer. The stirring was so intensive that the current was independent of the stirring rate. Figure 3 shows that spectra recorded at a given potential in the presence and absence of suspended SiC particles are very similar.

The spectra obtained at potentials more anodic than approximately -0.68 V corresponded to the spectrum generated by the EEC shown in Figure 4(a), whereas the spectra taken at potentials more cathodic than approximately -0.72 V were similar that generated by the EEC in Figure 4(b). The change from the inductive to capacitive behaviour was sharp and occurred over a relatively narrow range of potentials. The analysis presented by Cao [44] indicates that both EECs describe the same reaction mechanism, however with different values for parameters such as reaction rate constants, Tafel coefficients, surface coverages etc.

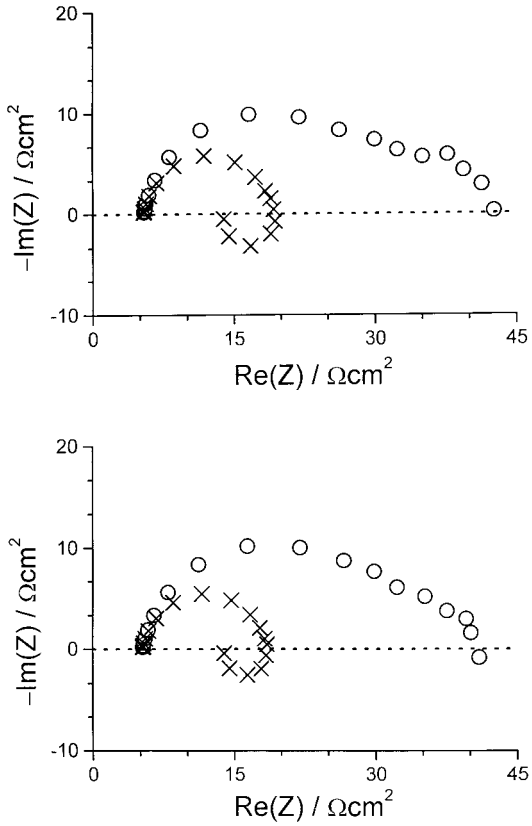

Fig. 3. Impedance spectra (20 frequencies between 65 535 and 0.125 Hz in logarithmic steps) for a nickel electrode in particle-free nickel Watts bath (upper) and in a Watts bath with 100 g dm^{-3} SiC (lower), at the *IR* corrected potentials of -0.728 V (×) and -0.688 V (○). Stainless steel disc cathode of 1.06 cm^2, $t = 55$ °C, pH 3.

For the analysis of the impedance data, the capacitance of the double layer (C_{dl}) in the EEC's was replaced by a constant phase element (CPE) [45]. It is generally believed that the origin of the CPE behaviour lies in the roughness and/or inhomogeneity of the electrode sur-

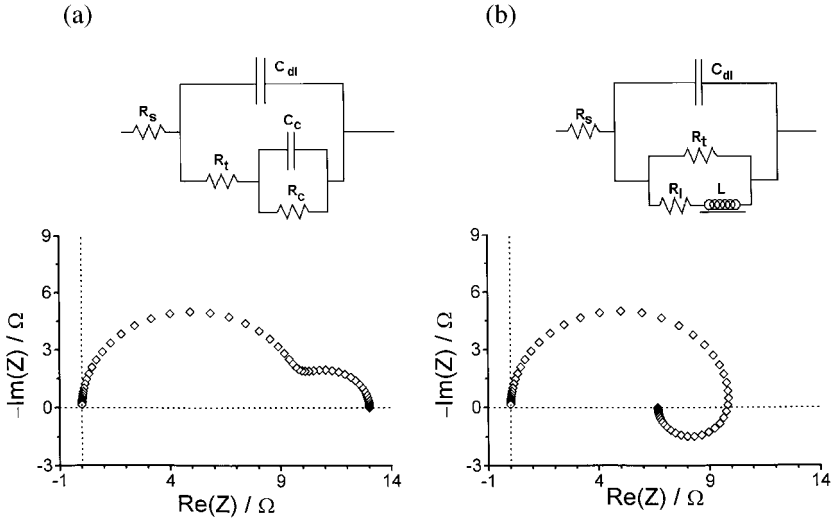

Fig. 4. Two equivalent electrical circuits (a, b) used to describe a nickel electrode in a plating bath. The impedance plots generated by these circuits are also shown. Values assumed in the simulation: $R_s = 0\ \Omega$, $C_{dl} = 100\ \mu F$, $R_t = 10\ \Omega$, $R_c = 3\ \Omega$, $C_c = 10$ mF, $R_l = 20\ \Omega$, $L = 1$ H.

face. The CPE model is assumed in this paper to describe the impedance of the electrolyte/Ni interface:

$$Z = \frac{1}{K}(j\omega)^{-\alpha} = \frac{\omega^{-\alpha}}{K}\cos(\alpha\pi/2) - j\frac{\omega^{-\alpha}}{K}\sin(\alpha\pi/2) \quad (2)$$

with K and α frequency independent constants. The factor K depends on the electrolyte concentration and is connected to the specific electrode capacitance. The factor α ($0.5 < \alpha < 1.0$) is thought to be characteristic for a given interface and independent of the electrolyte concentration. For electrodes showing a CPE behaviour, the electrode capacitance is different at each frequency and the capacitance of two electrodes may be compared only if both electrodes show the same value of α. To overcome that difficulty, Brug and coworkers [46] proposed for an electrode with faradaic current, the following equation to calculate the mean (or corrected) capacitance:

$$C_{corr} = \frac{K^{1/\alpha}}{\left(R_s^{-1} + R_t^{-1}\right)^{(1-\alpha)/\alpha}} \quad (3)$$

with R_t the charge transfer resistance and R_s the solution resistance. This equation is correct as long as the CPE concept is valid.

The EEC were fitted to the impedance data using the least-squares regression analysis program MINUIT [47]. The minimized function was

$$\sum\left[\frac{\mathrm{mod}(Z_{meas} - Z_{calc})}{\mathrm{mod}(Z_{meas})}\right]^2 \quad (4)$$

with summation over all frequencies. The square root of the calculated sum of squares in Equation 4 divided by the number of frequency points gave the mean relative error of the fit. All parameters appearing in the equation describing the EEC from Figure 4(b) were optimized. The mean relative error of the fit in most cases was lower than 0.01. Examples of the fit are presented in Table 1.

Figure 5 compares the impedance spectra recorded before and after the addition of particles to the bath. The experiments were started in a pure bath (without particles) and nickel deposition was performed at constant potential. After the deposition of each 5 μm thick nickel layer, the impedance measurement was performed. When the layer attained a thickness of 20 μm, particles were added to the solution and spectra were registered after the deposition of another 5 μm thick layer. A low area electrode was used in that experiment to avoid changes of R_s due to the addition of particles to the baths. On addition of particles to the solution, the diameter of the activation semicircle changed slightly, but the addition of silica and silicon carbide particles have an opposite influence on the impedance spectrum. An apparent decrease in the charge transfer resistance takes place on addition of silica. This decrease is accompanied by an increase in current and EDL capacitance of the electrode. It

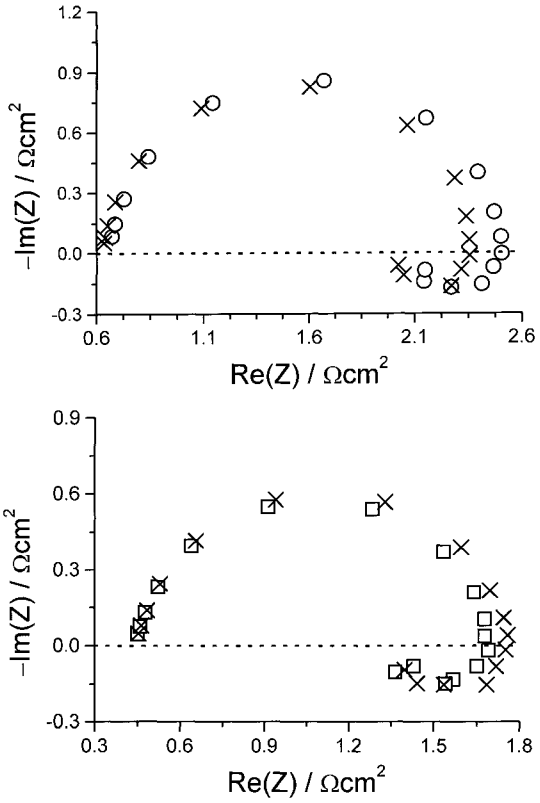

Fig. 5. Impedance spectra (17 frequencies between 65 535 and 1 Hz in logarithmic steps) before (+) and after the introduction of 100 g dm^{-3} SiC (○) or 40 g dm^{-3} SiO_2 (□) particles to a Watts bath operated at pH 3 and 55 °C. Gold cathode of the diameter of 1 mm. Potential before introduction of particles −0.83 V (*IR* corrected).

Table 1. Impedance parameters during nickel deposition before and after the addition of particles to the Watts bath (pH 3, 55 °C) on an electrode of 1 mm diameter at the potential of −0.85 V

The EEC from Figure 4b is assumed in the calculation of parameters. C_{corr} was calculated from Equation 3. $C_{10\,000}$ and C_{100} mean capacitance calculated for the CPE model (Equation 2) at f = 10 000 Hz and f = 100 Hz, respectively

Type of particle	Concentration /g dm^{-3}	R_s /Ω cm^2	R_t /Ω cm^2	α	10^6 K*	R_1 /Ω cm^2	L /H cm^2	C_{corr} /μF cm^{-2}	$C_{10\,000}$ /μF cm^{-2}	C_{100} /μF cm^{-2}
SiC	0	0.63	1.75	0.961	110	6.05	0.21	74.0	71.6	85.7
	100	0.66	1.86	0.949	119	6.69	0.27	70.0	67.9	72.2
SiO_2	0	0.45	1.31	0.939	140	3.21	0.16	73.2	71.7	94.8
	100	0.45	1.22	0.943	142	3.59	0.16	77.6	76.0	98.8

* The dimension of K depends on the value of α and may be deduced from Equation 2. For $\alpha \simeq 1$, $\sin(\alpha\,\pi/2)$ is close to 1 and K is equal to the capacitance of the electrode at a frequency of $1/2\pi$ Hz

suggests an increase in the surface roughness of the electrode. Such an increase in current after introduction of solid particles to the solution was reported [48] for TiO_2/Ni and ascribed to the catalytic action of particles on the nickel reduction. Also Watson [26] observed an increase in current for SiC/Ni and ascribed it to the increase in surface area of the electrode.

In the case of SiC particles the observed increase in charge transfer resistance was accompanied by the decrease in current and EDL capacitance, which suggests the decrease in electrode surface area. It was really observed in our previous work [42] that the Ni layers deposited in the presence of suspended SiC particles showed increased roughness.

Similar experiments were performed using the electrode with a higher (1.06 cm^2) surface area cathode. The main change observed in the spectrum on addition of SiO_2 to the bath was a horizontal shift of the whole spectrum (Figure 6) due to the increase in solution resistance. This may be explained assuming that some decrease in charge transfer resistance due to particle introduction (Figure 5) was compensated by an increase in charge transfer resistance due to the decrease in overpotential, caused by the increase of the *IR* potential drop. The parameter α was almost constant during deposition (Figure 6, lower part), whereas the parameter K increased on introduction of particles.

The opposite tendency was observed with silicon carbide particles (Figure 7), similarly to the experiment presented in Figure 5. A decrease in current (which was, however, caused partially by the increase in solution resistance) was accompanied by an increase in R_t. At the same time, a decrease in C_{corr} was noticed which suggests a decrease in the surface area of the electrode. This was, however, due to a change in α, not in K. Thus, it may be stated that the presence of particles being embedded in the surface increases the surface inhomogeneity. Also the presence of SiC in the nickel deposit makes the microscopic current distribution over the surface more uneven, which leads to a decrease of α. To check whether this was a regular trend or only a coincidental result, a series of measurements was performed in which Ni/SiC composites were deposited from baths with different particle concentrations. In each experiment the deposition was performed at a constant electrode potential, with the particles present in the plating bath right from the beginning of the experiments. The impedance spectra were recorded at intervals corresponding to 5 μm increases in layer thickness. The electrode capacitance calculated from Equation 3 for a layer of 20 μm thickness is plotted in Figure 8 against

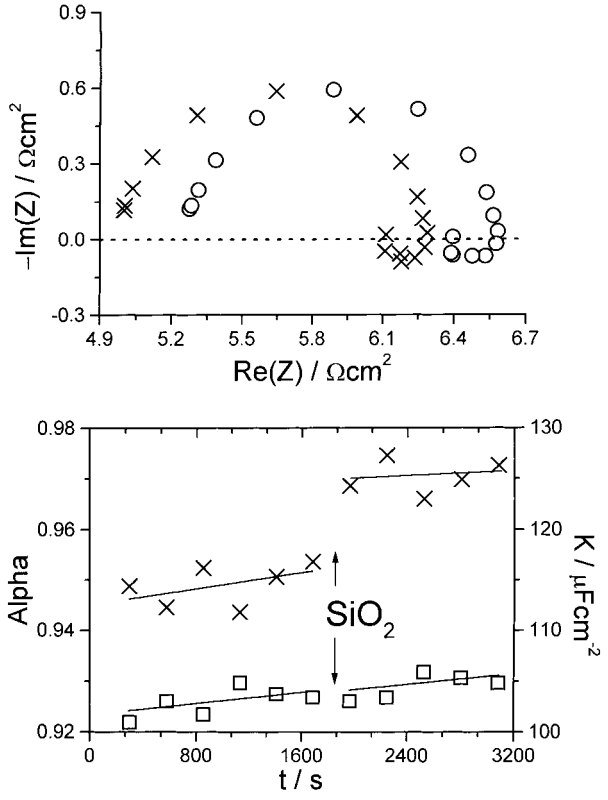

Fig. 6. Impedance spectra (17 frequencies between 65 535 and 1 Hz in logarithmic steps) before (×) and after (○) the introduction of SiO_2 particles to the Watts bath operated at pH 3 and 55 °C. Potential (*IR* corrected) before the introduction of particles –0.83 V. Steel electrode of 1.06 cm^2. In the bottom part of the figure the changes of the impedance parameters α (□) and K (×) during the electrolysis are shown (see Equation 2 for definition). Spectra performed at the 5 μm intervals of the Ni layer thickness.

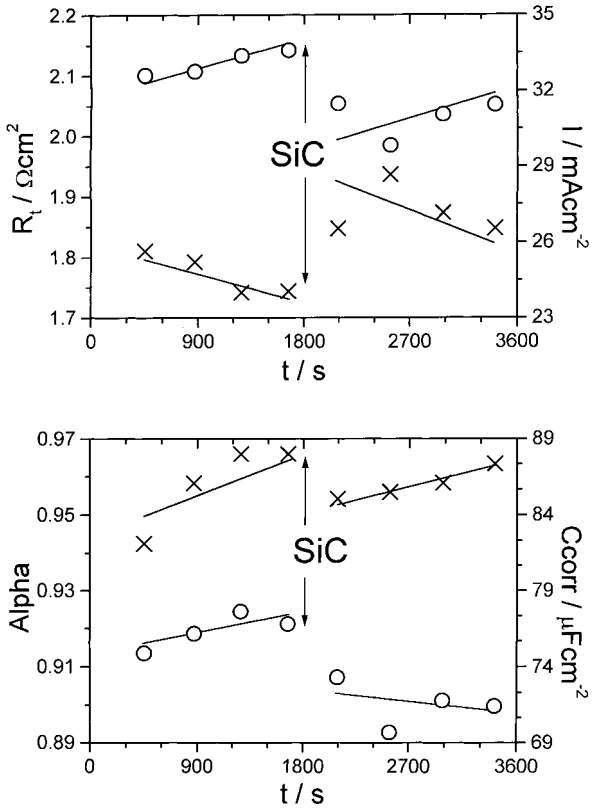

Fig. 7. Changes in current and impedance parameters due to the addition of SiC particles to the nickel Watts bath operated at pH 3 and 55 °C, for the experiment shown in Figure 5, C_{corr} values are calculated according to Equation 3. Spectra performed at the 5 μm intervals of the Ni layer thickness.

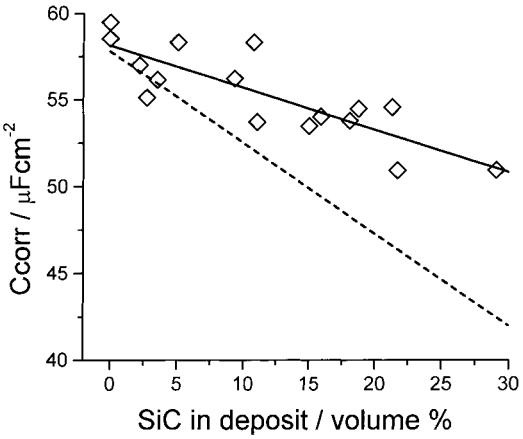

Fig. 8. Dependence of the corrected capacitance of the SiC/Ni electrode after the deposition of 20 μm Ni layer, calculated from Equation 3, on the SiC content in the composite coatings. Deposition conditions like in Figure 1.

the volume percent SiC in the composite coating. Despite the large scatter in the results, the correlation between C_{corr} and the SiC content in the composite reveals a decrease in capacitance at increasing content of SiC in the composite coatings (correlation coefficient -0.84). The observed decrease in calculated capacitance was, however, much lower than expected assuming a decrease in capacitance proportional to the volume content of SiC in the composite. Most probably there are two trends. The presence of SiC particles in the solution causes an increase in surface roughness, as suggested in the case of SiO_2, and on the other hand, particles partly embedded in the metal deposit block part of the surface.

4. Discussion

The changes in impedance parameters after the introduction of particles to the solution are given in Table 1: the relatively high value of α in the deposition experiments is clear. For the electrode of diameter 1 mm α attained a value between 0.92 and 0.98. Such a value was noticed, for example, in the case of polycrystalline Pt electrode [49] and indicates a relatively low dispersion of the electrode capacitance versus frequency. This may be connected with the fact that the nickel reduction is relatively slow, and occurs at high overvoltage, which reduces the inhomogeneity in current flow due to the primary and secondary current distributions. The CPE behaviour of the electrode is evidently influenced by the macroscopic nonuniform current distribution. For the larger electrode, α was always lower and the C_{corr} was always slightly lower in comparison to a smaller electrode operated under comparable conditions. It may also be ascribed to the influence of the macroscopic nonuniform current distribution on the capacitance of the EDL. Such a behaviour may be expected from Newman's treatment of the capacitance of a disc electrode [50].

The impedance parameters are not greatly affected by the introduction of particles to the solution, except the trivial influence on R_s, observable in the case of the electrode of the higher surface area (Figure 6). Yeh and Wan [27] observed a significant change in the adsorption pseudocapacitance of the electrode reaction due to the presence of particles in the solution. In our experiments, the changes in impedance parameters connected to the adsorption step (R_1 and L) on addition of particles to the solution, are comparable to the spread between consecutive measurements on the same electrode (Table 1). A well defined trend was not observed. When particles are codeposited, the reduction in the surface area of the electrode causes some increase in R_t (Table 1) and should cause a similar change in the parameters characterizing the adsorption step. Last, but not least, the introduction of particles to the solution may be accompanied by the introduction of impurities, which influence the coverage of the electrode by adsorbed intermediates. The conclusion of Yeh and Wan [27] that the impedance parameters of the electrode reaction reflect the participation of species adsorbed on the surface of particles in the electrode reaction cannot be confirmed. In the case of micrometre-sized particles, negligibly small amounts of ions are adsorbed on the surface in comparison to the amount of ions present in the layer of electrolyte of the same thickness as the particle diameter, adjacent to the electrode surface. So, it is rather doubtful that the current connected with the reaction of such small amounts contributes to a measurable extent to the electrode reaction. We also cannot confirm the large influence of the presence of SiC particles in the plating bath on the impedance of the nickel electrode during nickel electrocrystallization, observed by Benea and Carac [34].

The calculated electrode capacitance (Table 1 and Figures 7 and 8) seems to be reasonable in view of the data obtained for other polycrystalline metal electrodes [51] and is in reasonable agreement with earlier papers [28–33] concerning nickel electrode.

A reduction in electrode capacitance was not observed in the case of SiO_2 particles, which were embedded in the electrodeposited layer to a very limited extent (see Figure 1). This means that particles which do not embed, are separated from the electrode by a gap larger than the EDL thickness. Of course there is the possibility, that SiO_2 particles do block some part of the electrode surface, but the resulting decrease in electrode capacitance is overcompensated by the increase in surface roughness. However, analysis of the results does not support this view. In the case of the 100 g dm^{-3} SiC suspension the expected decrease in capacitance (Figures 1 and 8) was about 12 μF cm^{-2}. The observed value was only 6 μF cm^{-2}, about half of the expected value, supposedly due to the increase in surface roughness factor. It may be seen in Table 1 that the increase in capacitance in the case of SiO_2 suspension was very close to that value. Assuming that the presence of SiC and SiO_2 causes the same increase in electrode roughness it

may be concluded that either no blocking is observed for the case of SiO_2 or that the effect is negligibly small.

The difference in the codeposition rate between silica and silicon carbide still needs to be explained. According to the XPS results of Yeh and Wan [27], SiC conditioned in an aqueous solution is covered by a few nanometre thick layer of silica. Also the data of Maurin and Lavanant [35] on the surface analysis of SiC powders, suggest that the surface of SiC is covered by a layer of silica. Yeh and Wan [27] established the point of zero charge of SiC to be 2.2, very close to the point of zero charge of silica [52]. However, the presence of silica at the surface of SiC does not mean that both substances show the same hydrophobicity. The hydrophobicity of many solid materials was investigated by Drzymała [53]. The collectorless flotability was chosen by Drzymała to characterise the hydrophobicity of a material and it was found that SiO_2 is hydrophilic whereas SiC is hydrophobic. Flotation is similar to codeposition since in both processes a solid particle approaches an interface and the rupture of the aqueous film between the particle and the interface must occur to allow the capturing of particles at the interface. This is probably the main reason for the different behaviour of the two substances in codeposition, as already suggested by Fransaer et al. [22].

5. Conclusions

The EIS results suggest that particles suspended in a plating bath increase the roughness of the electrode surface. Silica, which hardly codeposits, increases the specific electrode capacitance while silicon carbide which codeposits easily, decreases the electrode capacitance, but to a lower extent than expected on the basis of the percentage of embedded particles. It is assumed that the lowering of the surface area of the electrode by partly embedded particles is counterbalanced to some extent by an increase in surface roughness. Indeed on addition of silica particles an apparent increase in surface roughness is the only effect detected. Blocking of the electrode by silica particles was not observed.

The EIS results suggest that particles adsorbed on but not embedded in the electrode, remain separated from that electrode surface by a liquid film thicker than the width of the electrical double layer. The rupture of that liquid film thus seems to be the key factor controlling the electrolytic codeposition of particles.

Acknowledgements

This work was financially supported by the European Community, COPERNICUS Program, Contract CIPA-CP-94-0225. Part of this work was also supported by Belgian Government within the Interuniversity Poles of Attraction (contract IUAP/P4/33). Dr Jan Fransaer wishes to thank the FWO-Vlaanderen for a post-doctoral grant.

References

1. J.C.Withers and E.F. Abrams, *Plating* **55** (1968) 605.
2. T.W. Tomaszewski, L.C. Tomaszewski and H. Brown, *Plating* **56** (1969) 1234.
3. C. Buelens, J. Fransaer, J.-P. Celis and J.R. Roos, *Bull. Electrochem.* **8** (1992) 371.
4. E.P. Rajiv and S.K. Seshadri, *Bull. Electrochem.* **8** (1992) 376.
5. R.S. Saifullin, 'Electrochemical Composite Coatings' (Khimiya, Moscow, 1972).
6. R.S. Saifullin, *Zh. Prikl. Khimi* **39** (1966) 810.
7. K. Helle, Proceedings 4th International Conferenc on 'Org. Coating Sci. and Technol.' **2** (1982) p. 264.
8. A. Hovestad and L.J.J. Janssen, *J. Appl. Electrochem.* **25** (1995) 519.
9. W. Metzger, R. Ott, G. Laux and H. Harst, *Galvanotechnik* **61** (1970) 998.
10. J.C. Withers, *Prod. Fin.* **8** (1962).
11. P.W. Martin, *Met. Finish. J.* **11** (1965) 399.
12. D.W. Snaith and P.D. Groves, *Trans. Inst. Metal. Finish.* **50** (1972) 95.
13. T.W. Tomaszewski, *Trans. Inst. Met. Finish.* **54** (1976) 45.
14. N. Guglielmi, *J. Electrochem. Soc.* **119** (1972) 1009.
15. J. Foster and A.M.J. Kariapper, *Trans. Inst. Met. Finish.* **51** (1973) 27.
16. J.M. Sykes and D.A. Alnert, *Trans. Inst. Met. Finish.* **51** (1973) 171.
17. A.M.J. Kariapper and J. Foster, *Trans. Inst. Met. Finish.* **52** (1974) 87.
18. M.J. Bhagwat, J.-P. Celis and J.R. Roos, *Trans. Inst. Met. Finish.* **61** (1983) 72.
19. R.S. Saifullin, R.N. Salakhiev and R.S. Kuramshin, *Kolloidn. Zh.* **50** (1988) 293.
20. B. Szczygiel, *Trans. Inst. Met. Finish.* **73** (1995) 142.
21. J.-P. Celis, J.R. Roos and C. Buelens, *J. Electrochem. Soc.* **134** (1987) 1402.
22. J. Fransaer, J.-P. Celis and J.R. Roos, *J. Electrochem. Soc.* **139** (1992) 413.
23. V.E. Shubin and P. Kékicheff, *J. Colloid. Interface Sci.* **155** (1993) 108.
25. S.W. Watson and R.P. Walters, *J. Electrochem. Soc.* **138** (1991) 3633.
26. S.W. Watson, *J. Electrochem. Soc.* **140** (1993) 2235.
27. S.H. Yeh and C.C. Wan, *J. Appl. Electrochem.* **24** (1994) 993.
28. A.J. Arvia and D. Posadas, *in* 'Encyclopedia of Electrochemistry of the Elements', edited by A.J. Bard, Vol. 3 (Marcel Dekker, New York, 1975).
29. I. Epelboin, M. Joussellin and R. Wiart, *J. Electroanal. Chem.* **119** (1981) 61.
30. E. Chassaing, K. Vu Quang and R. Wiart, *J. Appl. Electrochem.* **17** (1987) 1267 and **19** (1989) 839.
31. E. Chassaing and R. Wiart, *J. Electrochem. Soc.* **118** (1971) 1577.
32. O. Volk and H. Fisher, *Electrochim. Acta* **4** (1961) 251.
33. S.S. Krugliakov, N.T. Kudryavtsev and R.P. Sobolev, *Electrochim. Acta* **12** (1967) 1263.
34. L. Benea and G. Carac, *Cercet. Metal. Noi. Mater.* **5** (1997) 20.
35. G. Maurin and A. Lavanant, *J. Appl. Electrochem.* **25** (1995) 1113.
36 B. Szeptycka, *Inz. Powierzchni* **4** (1997) 45.
37. M. Kimoto, A. Yakawa, T. Tsuda and R. Kammel, *Metall.* **44** (1990) 1148.
38. M. Ramasubramanian, S.N. Popova, B.N. Popov, R.E. White and K.-M. Yin, *J. Electrochem. Soc.* **143** (1996) 2164.
39. R.S. Saifullin, R.E. Fomina and A.R. Saifullin, *Zashch. Met.* **4** (1986) 611.
40. D. Aslanidis, J. Fransaer and J.-P. Celis, *J. Electrochem. Soc.* **144** (1997) 2352.
41. Y. Shiohara, A. Okado, M. Abe and M. Sagiyama, *Tetsu-to-Hagane* **77** (1991) 878.
42. C. Dedeloudis, M.K. Kaisheva, N. Muleshkov, T. Muleshkov, P. Nowak, J. Fransaer and J.P. Celis, *Plat. Surf. Finish.*, **86**(8) (1999) 57.

43. J. Newman, *J. Electrochem. Soc.* **113** (1966) 501.
44. Chu-nan Cao, *Electrochim. Acta* **35** (1990) 831 and **35** (1990) 837.
45. L. Nyikos and T.Pajkossy, *Electrochim. Acta* **30** (1985) 1553.
46. G.J. Brug, A.L.G. Van den Eeden, M. Sluyters-Rehbach and J.H. Sluyters, *J. Electroanal. Chem.* **176** (1984) 275.
47. CERN Computer Centre Program Library, D506.
48. G.N.K. Ramesh Babu, V.S. Muralidharan and F. Rodriguez-Reinoso, *Plat. Surf. Finish.* **78** (1991) 126.
49. T. Pajkossy, *J. Electroanal. Chem.* **364** (1994) 111.
50. J. Newman, *J. Electrochem. Soc.* **117** (1970) 198.
51. M.A. Vorotyntsev, *in* 'Modern Aspects of Electrochemistry' Vol. 17, edited by, B.E. Conway, R.E. White and J.O'M. Bockris (Plenum, New York, 1986), p. 131.
52. G.A. Parks, *Chem. Rev.* **65** (1965) 177.
53. J. Drzymała, *Int. J. Mineral Process.* **42** (1994) 139 and **42** (1994) 153.